Available online at www.sciencedirect.com
SCIENCE DIRECT®
Journal of Organometallic Chemistry 689 (2004) 1425–1430
Journal of Organometallic Chemistry
www.elsevier.com/locate/jorganchem

Structural and mechanistic studies on ion insertion into the molecular box $\{[CpCo(CN)_3]_4[Cp^*Ru]_4\}$

Maya Ramesh, Thomas B. Rauchfuss *

Department of Chemistry, University of Illinois at Urbana – Champaign, Urbana, IL 61801, USA

Received 9 December 2003; accepted 11 February 2004

Abstract

The molecular box $[CpCo(CN)_3]_4[Cp^*Ru]_4$ (Co_4Ru_4) reacts readily with a variety of monocations to form $M\subset Co_4Ru_4^+$ ($M = K^+$, Cs^+, Rb^+). Ion competition experiments, monitored by ESI-MS, show that the molecular box binds the smaller K^+ more rapidly than Cs^+, but that thermodynamically Co_4Ru_4 prefers the larger ion. The rates of ion-insertion for K^+ and Cs^+ into Co_4Ru_4 were found to qualitatively follow second order kinetics with K^+, 300 M^{-1} s^{-1} and Cs^+, 36 M^{-1} s^{-1}. The ratio k_K/k_{Cs} qualitatively matched the ESI-MS results from ion competition experiments. The rates of ion-insertion into Co_4Ru_4 were found to depend on the counter anions. In particular, $RbBF_4$ reacted with Co_4Ru_4 more slowly than did RbOTf. The slower rates allowed us to establish second order kinetics. ^1H NMR studies reveal that the Cp signal for Co_4Ru_4 is very sensitive to the presence of entering ions, e.g., Rb^+, whereas the corresponding Cp signal for $Rb\subset Co_4Ru_4^+$ was insensitive to the presence of Rb^+. The molecular structures of $[Co_4Ru_4]\cdot 6MeCN$, $[K\subset Co_4Ru_4]BF_4\cdot 7MeCN$, $[Cs\subset Co_4Ru_4]BF_4\cdot 6MeCN$ and $[Tl\subset Co_4Ru_4]BF_4\cdot 6MeCN$, determined by X-ray diffraction, showed that although the compounds crystallized in the same space group *I*23, a correlation exists between the Ru–N/Co–C bond distances and the size of the interstitial ion.

Keywords: Cyanide; Cyclopentadienyl; Cobalt; Cage; Molecular ionophilic box; Ion-insertion; Kinetics

1. Introduction

Molecular containers are the smallest possible agents for sensing, sorting, and sequestering ions and molecules [1,2]. It therefore seems very likely that future devices will exploit the host–guest behavior of such molecular objects. The inspiration for molecular containers discussed in this paper Prussian Blue (PB) and its variants, are in fact polymers with box-like subunits that give rise to ion-exchange behavior [3]. Our work has aimed at replicating cubic and related frameworks that resemble subunits of the PB structure [4,5]. Gratifyingly, some such species exhibit highly selective ionophilicities [6]. The charge on the cage appears to be key to the ionophilicity. Anionic cages, e.g., $\{M\subset[Cp^*Rh(CN)_3]_4[Mo(CO)_3]_4\}^{3-}$ [7], have only been isolated with an interstitial alkali metal ion, suggesting that the interstitial ion is required for their existence although these species do undergo ion exchange reactions.

In contrast to anionic cages, cationic derivatives, e.g., $\{[CpCo(CN)_3]_4[Cp^*Rh]_4\}^{4+}$[4], exhibit no affinity for cations (or anions). Recently, however, we have been able to prepare neutral boxes, the prototype being $\{[CpCo(CN)_3]_4[Cp^*Ru]_4\}$ (Co_4Ru_4) [8]. This species forms via the $EtNH_3^+$-templated reaction of the constituent organometallic building blocks (Eq. (1))

$$4PPN[CpCo(CN)_3] + 4[Cp^*Ru(NCMe)_3]PF_6 \xrightarrow{EtNH_3BF_4} \underset{Co_4Ru_4}{\{[CpCo(CN)_3]_4[Cp^*Ru]_4\}} + 4PPNPF_6 \quad (1)$$

We propose that the bulky alkylammonium ion stabilizes intermediates in the cage assembly process but is too large to be incorporated into the completed box. The isolability of this cage in its voided form is

* Corresponding author. Tel.: +2173335070; fax: +2173332685.
E-mail address: rauchfuz@uiuc.edu (T.B. Rauchfuss).

0022-328X/$ - see front matter © 2004 Elsevier B.V. All rights reserved.
doi:10.1016/j.jorganchem.2004.02.028

attributed to its neutral charge, which reduces its ionophilicity. Despite its charge neutrality, Co_4Ru_4 is still a strong ionophore binding numerous monocations (Eq. (2))

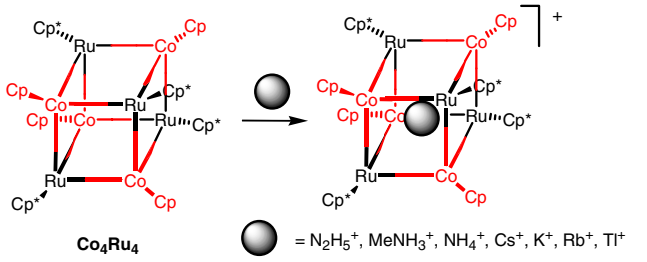

(2)

The easy ion-binding and ion-exchange properties of Co_4Ru_4 prompted us to probe certain details of the ion binding process. Furthermore, we disclose the crystallographic characterization of Co_4Ru_4 as well as the alkali metal-containing products. These studies are fundamentally relevant to understanding the behavior of PB analogs and the design of new ion sequestering agents [3].

2. Results

2.1. Qualitative studies on ion binding by Co_4Ru_4

We begin with ion competition experiments, whereby Co_4Ru_4 is treated with a mixture of alkali metal ions and the resulting solution is examined by ESI-MS without any work-up. In this way, the affinity of the box for the ions could be probed. Reactions were conducted in a mixed solvent of MeCN and THF, which allowed these reactions to be monitored in homogeneous solutions (Co_4Ru_4 is insoluble in MeCN, the solvent of choice for the metal cations). We employed a 2*x* excess of the cations. As shown in Fig. 1, K^+ inserts rapidly into Co_4Ru_4 but is subsequently displaced by Cs^+ to give $[Cs\subset Co_4Ru_4]^+$.

The rate of insertion of ions into Co_4Ru_4 is consistent with second-order kinetics. Because the rates were too fast to be monitored under pseudo-first order conditions, we examine the reaction under the condition where $[M^+]_0 = [Co_4Ru_4]_0$ by monitoring the ^1H NMR signals for C_5H_5. The kinetic analysis allowed us to estimate rate constants from these otherwise rapid reactions. The time dependence of these reactions is poorly fit to linearity (Fig. 2), which may be due to low precision in measuring the reactants and other interfering effects, such as inhomogeneous mixing (see Section 4). Despite these problems, the relative rates of ion insertion can be gleaned from the initial rates. Furthermore, the ratio k_K/k_{Cs} is consistent with the ratio of the ion currents in Fig. 1.

2.2. Kinetics of insertion of Rb^+ into Co_4Ru_4

The counter anions were found to significantly affect the rate of ion insertion. For example, $RbBF_4$ inserts noticeably more slowly than the corresponding RbOTf, both in MeCN solution. The rate of reaction of $RbBF_4$ and Co_4Ru_4 was sufficiently slow that we were able to monitor the kinetics by NMR spectroscopy under conventional pseudo-first order conditions, using excess Rb^+ (Figs. 3 and 4). The quality of this fit indicates that indeed Rb^+ inserts via a bimolecular process.

2.3. NMR evidence for ion-preassociation with Co_4Ru_4

^1H NMR spectra of the reaction mixture reveal that Co_4Ru_4 significantly interacts with Rb^+. In particular, the chemical shift for the Cp groups on Co_4Ru_4 move by ~0.1 ppm as Rb^+ is consumed in the ion insertion

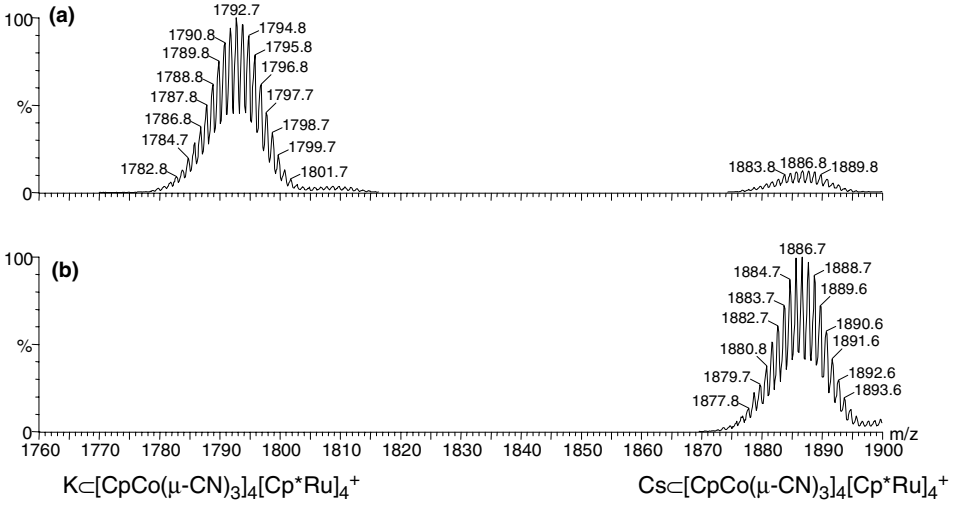

Fig. 1. ESI-MS spectra of a 5.7×10^{-3} M THF solution Co_4Ru_4 to which a 1.14×10^{-2} M in KPF_6 and CsOTf in MeCN solution was added; after 10 min (a) and after seven days (b) at 25 °C.

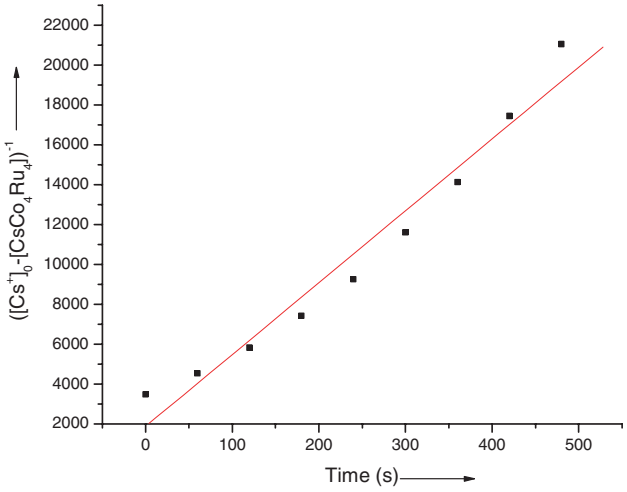

Fig. 2. Graph of $([Cs^+]_0\text{-}[Cs\subset Co_4Ru_4^+])^{-1}$ vs. time, allowing an estimation of k_1. The straight line corresponds to $k_1 = 36\ M^{-1}\ s^{-1}$. Conditions: $[Co_4Ru_4]_0 = [Cs^+]_0 = 1.63 \times 10^{-3}$ M in 1:1 mixture of CD_3CN and d_8-thf, 25 °C. The curvature indicates that the reaction is accelerating over the course of the reaction.

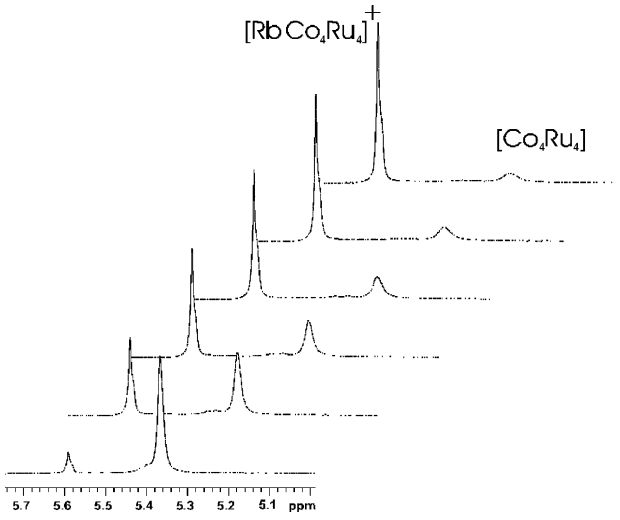

Fig. 3. 500 MHz ^{1}H NMR spectra for stages in the reaction of Co_4Ru_4 and RbOTf in THF:CD_3CN. $[Rb^+]_0 = [Co_4Ru_4]_0 = 0.00163$ M.

process (see Fig. 3). In the case of Cs^+ ion insertion, the corresponding shift was ca. 0.3 ppm. It can also be seen that the ^{1}H NMR chemical shifts for $Rb\subset Co_4Ru_4^+$ are unaffected by $[Rb^+]$, consistent with the reduced affinity of the cationic "filled" box for Rb^+ (see Table 1).

2.4. Crystallographic studies

The solid state structures of the empty cage Co_4Ru_4 and two of its derivatives were examined by X-ray crystallography. The salts are isostructural, crystallizing in the cubic space group $I23$. $I23$ symmetry was imposed on the box framework. Cp and Cp* ligands were refined as idealized rigid groups disordered about three-fold symmetry axes. A comparison of the bond distances and angles

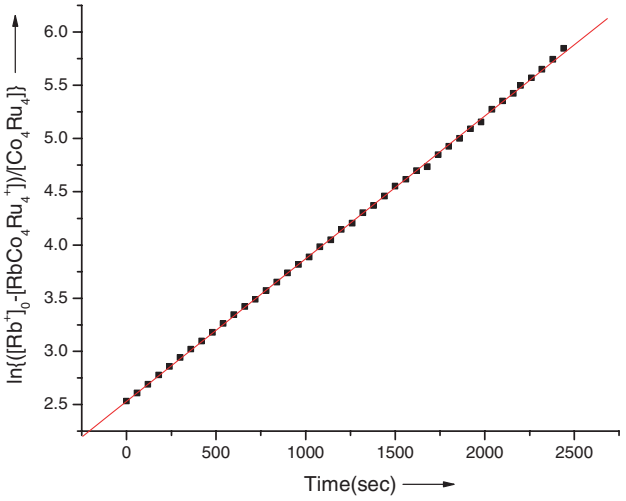

Fig. 4. Pseudo-first kinetic analysis of the reaction of $RbBF_4 + Co_4Ru_4$; $[Rb^+]_0 = 10[Co_4Ru_4] = 0.0163$ M. The reaction was conducted in 1:1 solvent mixture CD_3CN and d_8-thf, 25 °C.

Table 1
Approximate rate constants for insertion of various alkali metal ions into Co_4Ru_4 at 25 °C

MX	Ionic radius of M^+ (pm)	k_1 ($M^{-1}\ s^{-1}$)
KOTf	138	300
$RbBF_4$	152	1.8
CsOTf	167	36

(Table 2) reveals that the distortion of the cage structure from idealized cubic framework is affected by the interstitial ion. The distortions are manifested in the Co1–C1–N1 and Ru1–N1–C1 angles, with the K^+ derivative being more distorted than the Cs^+ derivative (Table 2).

The geometry of the cages Co_4Ru_4 and $[Cs\subset Co_4Ru_4]$ may be described as nearly idealized cubes (Fig. 5). The Co–C and Ru–N distances in Co_4Ru_4 and $[Cs\subset Co_4Ru_4]BF_4$ are 1.878(4) vs. 1.900(9) Å and 2.087(3) vs. 2.065(8) Å, respectively. The maximum deviation of all Co–C–N and Ru–N–C angles from linearity was 176.5(9)° for the Ru–N–C angle in $[Cs\subset Co_4Ru_4]BF_4$, which is certainly due to the attractive interaction between Cs^+ ion and the CN ligands.

Table 2
Comparison of bond parameters for Co_4Ru_4 and the "filled" boxes $[Cs\subset Co_4Ru_4]BF_4$ and $[K\subset Co_4Ru_4]BF_4$

Parameters	$[Cs\subset Co_4Ru_4]BF_4$	$K\subset Co_4Ru_4BF_4]$	Co_4Ru_4
Co1–M (Å)	4.376	4.347	
Ru1–M (Å)	4.451	4.451	
N1–M (Å)	3.585(8)	3.580	
C1–M (Å)	3.625(8)	3.660	
C1–N1 (Å)	1.134(7)	1.207(15)	1.131(5)
C1–Co1 (Å)	1.900(9)	1.861(15)	1.878(4)
N1–Ru1 (Å)	2.065(8)	2.017(12)	2.087(3)
Co1–C1–N1 (°)	178.8(10)	174.8(12)	179.9(4)
Ru1–N1–C1 (°)	176.5(9)	174.0(12)	178.5(3)

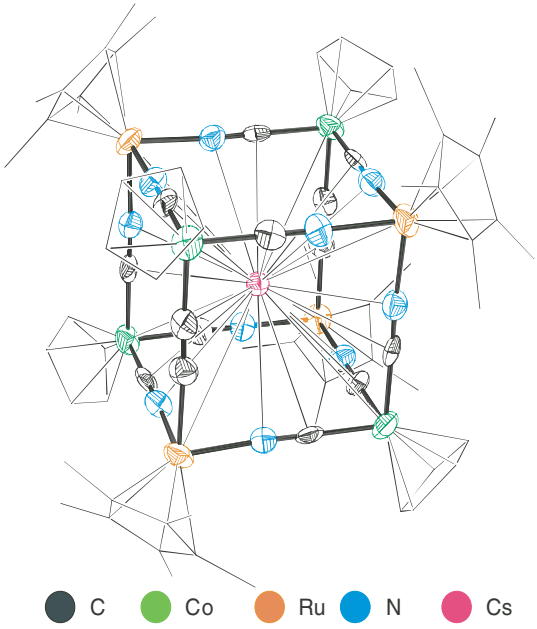

Fig. 5. Molecular cation of $[Cs\subset Co_4Ru_4]BF_4$ showing 35% thermal ellipsoids. Symmetry related positions were omitted to preserve clarity.

The structure of the "empty" box shows a residual 0.51 electron density at its crystallographic origin. Of course, further evidence for our claim that Co_4Ru_4 is indeed void is provided by the fact that it binds ions.

The Co–CN–Ru edges of the boxes with interstitial ions bow inward to interact with the ions, especially in $[K\subset Co_4Ru_4]^+$ as is demonstrated by the mean Co–C–N and Ru–N–C angle of 174.4° vs. 178.4° for $[Cs\subset Co_4Ru_4]^+$ and Co_4Ru_4.

All of the cages studied in this work (and in previous studies) exhibit the presence of MeCN solvent molecules positioned at each of the six square faces of the box. In each case, it is the CH_3 end of the solvate that is directed toward the cage face.

In the previously characterized cage $\{K\subset[Cp^*Rh(CN)_3]_4[Mo(CO)_3]_4\}^{3-}$, the alkali metal cation was found to be distributed over two equivalent, off-centered positions inside the box. In the case of $[K\subset Co_4Ru_4]^+$, the potassium is centered. We attribute this change in location to the smaller size of the Ru_4Co_4 box compared with the Mo_4Rh_4 species. A comparison of relevant cage dimensions is shown in Table 3.

The box volume may be relevant to the curious finding that the K^+ is centered in Co–Ru boxes but not in the larger Mo–Rh boxes. Further work is planned to examine other larger cages in an effort to further probe bistability in the binding of alkali metal cations.

3. Summary

Qualitative and quantitative rate measurements indicate that alkali metal cations insert via a bimolecular process. This finding implies that the box remains intact throughout the insertion. An alternative process would entail rate-determining opening of the cage followed by rapid uptake of the ion. Also arguing against this cage-opening mechanism is the low reactivity of these cages toward Et_4NCN – we would expect that partially open cages would be highly susceptible to degradation by cyanide.

One surprise from this work is the evidence for pre-association of the cations with the cage. In retrospect, this interaction was anticipated by the fact that all crystallographic characterizations revealed the presence of a MeCN adjacent to each $M_4(CN)_4$ face in all structural determinations. We have preliminary evidence for a particularly high affinity of the cages for ammonium ions, a property that might be useful in designing supramolecular systems based on box–H_3NR^+ interactions.

4. Experimental

4.1. Estimation of k_1 for the $Co_4Ru_4 + M^+$ reaction ($M = K$, Cs)

The rate constant for insertion of K^+ and Cs^+ into Co_4Ru_4, k_1, was analyzed under conditions where $[M^+]_0 = [M\subset Co_4Ru_4^+]$. Measurements were conducted at ambient conditions while maintaining uniformity in solvent and counterion (OTf^-), and concentration for all experiments.

$$\frac{d[M\subset Co_4Ru_4^+]}{dt} = k_1[M^+][Co_4Ru_4]$$
$$= k_1\{[M^+]_0 - [M\subset Co_4Ru_4^+]\}\{[Co_4Ru_4]_0 - [M\subset Co_4Ru_4^+]\}.$$

Putting $[M\subset Co_4Ru_4^+] = x$,

$$\frac{dx}{dt} = k_1(a-x)^2, \quad \text{where } [M^+]_0 = [Co_4Ru_4]_0 = a,$$

$$[M^+]_0 = [Co_4Ru_4]_0,$$
$$[Co_4Ru_4]_0 = [M\subset Co_4Ru_4^+]_t + [Co_4Ru_4]_t,$$
$$[M^+]_0 = [M^+]_t + [M\subset Co_4Ru_4^+]_t$$

Table 3
Comparison of cage dimensions in $\{K\subset[CpCoCpCo(CN)_3]_4\}PF_6$ and $(Et_4N)_3\{K[Cp^*Rh(CN)_3]_4[Mo(CO)_3]_4\}$

	$\{K\subset[CpCoCpCo(CN)_3]_4\}PF_6$	$(Et_4N)_3\{K[Cp^*Rh(CN)_3]_4[Mo(CO)_3]_4\}$
Cage sides	Co–Ru = 5.081 Å	Rh–Mo = 5.359(7) Å
Longest diagonal	Co–Ru = 8.799 Å	Rh–Mo = 9.250(6) Å
Face diagonal	Co–Co = 7.184 Å	Rh–Rh = 7.550(7) Å

Integrating

$$\frac{1}{a-x} = k_1 t + C, \quad \text{where } C \text{ is a constant.}$$

At $t = 0$, $C = \frac{1}{a}$. Therefore

$$\frac{1}{a-x} = k_1 t + \frac{1}{a}$$

$$\frac{1}{[M^+]_0 - [M \subset Co_4Ru_4^+]} = k_1 t + \frac{1}{[M^+]_0}. \quad (3)$$

4.1.1. Procedure

Stock solutions, 0.0114 M in MOTf (M = K, Cs) and 5.708×10^{-3} M in Co_4Ru_4 were prepared in 1:1 THF:CD_3CN. 0.2 ml of the Co_4Ru_4 solution was syringed into the NMR tube and the volume was made up to 0.5 ml with a 1:6 THF-d_8:CD_3CN solvent mixture. Then, 0.1 ml of the MOTf solution was syringed into the tube, which was shaken and then inserted into the NMR probe.

For the case of $[K \subset Co_4Ru_4^+]$, after 44 s the ^1H NMR signal for Co_4Ru_4 was found to be 5% of the intensity of the signal for $[K \subset Co_4Ru_4^+]$.

At $t = 44$ s; $[Co_4Ru_4] = 0.05[K \subset Co_4Ru_4^+]$. Also $[Co_4Ru_4]_0 = [K \subset Co_4Ru_4^+] + [Co_4Ru_4]$ Knowing that $[Co_4Ru_4]_0 = [K^+]_0 = 1.63 \times 10^{-3}$ M, so $[K \subset Co_4Ru_4^+]_{t=44\,s} = 1.56 \times 10^{-3}$ M. Now putting the above values in Eq. (3) (above) and solving for k_1, one obtains $k_1 = 300\ M^{-1}\ s^{-1}$.

For the case of $[Cs \subset Co_4Ru_4^+]$, a plot of $([Cs^+]_0 - [Cs \subset Co_4Ru_4^+])^{-1}$ vs. time gave $k_1 = 36\ M^{-1}\ s^{-1}$ (Fig. 2).

4.2. Determination of k_1 under pseudo first-order conditions for $[Rb \subset Co_4Ru_4^+]$

Stock solutions were 0.114 M in $RbBF_4$ and 5.708×10^{-3} M in Co_4Ru_4 in 1:1 THF:CD_3CN. 0.2 ml of the Co_4Ru_4 solution was syringed into the NMR tube followed by 0.5 ml 1:6 THF:CD_3CN mixture. To this solution was added via syringe 0.1 ml of the $RbBF_4$ solution. The NMR tube was shaken and then inserted into the NMR probe and the spectra were monitored at 1 min intervals.

4.3. Preparation of $[M \subset Co_4Ru_4]^+$ salts

The following preparation is illustrative. A mixture of 50 mg (0.028 mmol) of Co_4Ru_4 and 38 mg (0.11 mmol) of $TlPF_6$ in 20 ml of MeCN was stirred at room temperature for 24 h. On reduction of the solvent volume to ca. 10 ml, dark-red microcrystals of $[Tl \subset (CpCo)_4\ (Cp^*Ru)_4(CN)_{12}]PF_6$ formed, which were filtered and washed with ether. Yield: 35 mg (65%). ^1H NMR (CD_3CN): δ 1.680 (s, 60H), 5.570 (s, 20H). ESI-MS (m/z): 1956.

The preparation of Co_4Ru_4, $[Cs \subset Co_4Ru_4]OTf$ and $[K \subset Co_4Ru_4]PF_6$ has been described [8]. Similar preparative procedures were used for $[Rb \subset Co_4Ru_4]BPh_4$ and $[N_2H_5 \subset Co_4Ru_4]BF_4$ using RbOTf and $N_2H_5BF_4$, respectively. Characterization details for these species follow:

$[Cs \subset Co_4Ru_4]OTf$: ^1H NMR (CD_3CN): δ 1.672 (s, 60H), 5.571 (s, 20H). ESI-MS (m/z): 1885.

$[Rb \subset Co_4Ru_4]BPh_4$: ^1H NMR (CD_3CN): δ 1.681 (s, 60H), 5.568 (s, 20H). ESI-MS (m/z): 1837.

$[Tl \subset Co_4Ru_4]PF_6$: ^1H NMR (CD_3CN): δ 1.680 (s, 60H), 5.570 (s, 20H). ESI-MS (m/z): 1956.

4.4. Crystallography

Crystals of $[K \subset Co_4Ru_4]BF_4 \cdot 7MeCN$ and $[Cs \subset Co_4Ru_4]BF_4 \cdot 6MeCN$ were grown by slow diffusion of Et_2O into a MeCN solution of $EtNH_3BF_4$ and

Table 4
Crystal and crystallographic data collection details

Parameter	$[Co_4Ru_4] \cdot 6MeCN$	$[K \subset Co_4Ru_4]BF_4 \cdot 7MeCN$	$[Cs \subset Co_4Ru_4]BF_4 \cdot 6MeCN$
Chemical formula	$C_{84}H_{98}Co_4N_{18}Ru_4$	$C_{86}H_{101}BCo_4F_4KN_{19}Ru_4$	$C_{84}H_{98}BCo_4CsF_4N_{18}Ru_4$
Temperature (K)	193(2)	193(2)	193(2)
Crystal size (mm)	$0.64 \times 0.38 \times 0.34$	$0.21 \times 0.17 \times 0.12$	$0.25 \times 0.22 \times 0.17$
Space group	I23	I23	I23
$a = b = c$ (Å)	18.032(2)	17.9784(16)	17.995(3)
$\alpha = \beta = \gamma$ (°)	90	90	90
V (Å^3)	5863.6(12)	5811.0(9)	5827.3(17)
Z	2	2	2
$D_{calc.}$ (Mg m^{-3})	1.133	1.238	1.265
μ (Mo Kα, mm^{-1})	1.091	1.146	1.413
Minimum and maximum transitions	0.56694/0.74323	0.8674/0.7625	0.7567/0.6393
Reflections measured/independent	19 135/2381	13 041/1283	17 717/2016
Data/restraints/parameters	2381/261/172	1283/373/237	2016/354/212
Goodness-of-fit	1.191	1.046	1.009
R_1[a] $[I > 2\sigma]$ (all data)	0.0474(0.1387)	0.0920(0.2276)	0.0573(0.1409)
R_w[b] $[I > 2\sigma]$ (all data)	0.0623(0.1496)	0.1504(0.2628)	0.1087(0.1569)
Maximum peak/hole (e$^-$/Å^3)	0.849/−0.414	0.567/0.478	0.891/−0.509

[a] $R_1 = \sum [||F_o| - |F_c||] / \sum |F_o|$.

[b] $R_w = \left[w(|F_o| - |F_c|)^2 \right] / \sum \left[wF_o^2 \right]$.

$[M\subset Co_4Ru_4]X$ ($MX = KPF_6$, CsOTf). Crystallographic parameters are listed in Table 4.

Crystallographic data (excluding structure factors) for the structures reported in this paper have been deposited with the Cambridge Crystallographic Data Centre as Supplementary Publication Nos. CCDC-222206, 222207, and 222208.

Acknowledgements

The authors thank Dr. Sodio C.N. Hsu for preliminary experiments. This research was supported by the US Department of Energy.

References

[1] J.-M. Lehn, Supramolecular Chemistry, VCH, Weinheim, 1995.
[2] F. Vögtle, Supramolecular Chemistry, Wiley, New York, 1991.
[3] K.R. Dunbar, R.A. Heintz, Prog. Inorg. Chem. 45 (1997) 283–391.
[4] K.K. Klausmeyer, T.B. Rauchfuss, S.R. Wilson, Angew. Chem. Int. Ed. 37 (1998) 1808–1810.
[5] S.M. Contakes, K.K. Klausmeyer, R.M. Milberg, S.R. Wilson, T.B. Rauchfuss, Organometallics 17 (1998) 3633–3635.
[6] M.L. Kuhlman, T.B. Rauchfuss, J. Am. Chem. Soc. 125 (2003) 10084–10092.
[7] K.K. Klausmeyer, S.R. Wilson, T.B. Rauchfuss, J. Am. Chem. Soc. 121 (1999) 2705–2711.
[8] S.C.N. Hsu, M. Ramesh, J.H. Espenson, T.B. Rauchfuss, Angew. Chem. Int. Ed. 42 (2003) 2663–2666.